

Article

Quantized-Feedback-Based Adaptive Event-Triggered Control of a Class of Uncertain Nonlinear Systems

Yun Ho Choi  and Sung Jin Yoo * 

School of Electrical and Electronics Engineering, Chung-Ang University, 84 Heukseok-Ro, Dongjak-Gu, Seoul 06974, Korea; dbsh4302@cau.ac.kr

* Correspondence: sjyoo@cau.ac.kr

Received: 14 August 2020; Accepted: 15 September 2020; Published: 17 September 2020



Abstract: A quantized-feedback-based adaptive event-triggered tracking problem is investigated for strict-feedback nonlinear systems with unknown nonlinearities and external disturbances. All state variables are quantized through a uniform quantizer and the quantized states are only measurable for the control design. An approximation-based adaptive event-triggered control strategy using quantized states is presented. Compared with the existing recursive quantized feedback control results, the primary contributions of the proposed strategy are (1) to derive a quantized-states-based function approximation mechanism for compensating for unknown and unmatched nonlinearities and (2) to design a quantized-states-based event triggering law for the intermittent update of the control signal. A Lyapunov-based stability analysis is provided to conclude that closed-loop signals are uniformly ultimately bounded and there exists a minimum inter-event time for excluding Zeno behavior. In simulation results, it is shown that the proposed quantized-feedback-based event-triggered control law can be implemented with less than 10% of the total sample data of the existing quantized-feedback continuous control law.

Keywords: quantized feedback control; event-triggered; adaptive control; neural networks; unmatched nonlinear uncertainties

1. Introduction

As networked control systems including digital communication channels have been successfully utilized in various industrial applications, significant research efforts have been devoted to control designs using input and state quantization [1–3]. Concurrently, nonlinear systems have been widely studied and significant progress has been achieved in the analysis and the control of nonlinear systems. On the other hand, recursive control techniques have attracted much attention as effective ways for dealing with the unmatched nonlinearities of lower-triangular nonlinear systems [4–6]. Based on these recursive control techniques, adaptive control strategies were presented for input-quantized lower-triangular nonlinear systems with unknown parameters [7,8] and completely unknown nonlinearities [9–12]. Fundamentally, the controllers designed in [9–12] assume that state variables are continuously measurable. As opposed to the previous works [7–12] considering input quantization, the control design problem of state-quantized nonlinear systems in a lower-triangular form has received limited attention. In [13], an adaptive quantized feedback backstepping controller using quantized state variables was presented under the assumption that the partial derivatives of recursive virtual controllers were constants. Thus, the result [13] is only usable for systems with nonlinear functions matched to a control input. In order to overcome this restriction, an adaptive quantized feedback control design methodology adopting the command filtered backstepping technique for lower-triangular nonlinear systems was recently presented in [14]. Despite this progress, two aspects still need to be addressed to realize further improvement in the quantized feedback control design [14].

(P1) In the existing work [14], unmatched nonlinearities should be known and satisfy the Lipchitz condition with known Lipchitz constants. Thus, it is still necessary to determine a method to address completely unknown and unmatched nonlinearities in the quantized feedback tracker design of lower-triangular nonlinear systems.

(P2) The result [14] may be impractical for a network-based control implementation in limited network resources because the control law designed in [14] should be updated continuously in time. Thus, the event-triggered operation strategy of the quantized-feedback-based controller needs to be studied.

Emerging event-triggered methodologies for network-based control have received increasing attention in the control society because of limited communication bandwidths in networks [15,16]. Unlike the conventional time-triggered strategy, an event-triggered strategy can reduce the amount of computation and communication resources required in networked control systems. Owing to these advantages, some event-triggered control methods were presented for linear and nonlinear networked control systems [17–20]. For lower-triangular nonlinear systems with parametric uncertainties, Xing et al. [21] first suggested an adaptive recursive event-triggered control approach using three types of thresholds. Thereafter, numerous event-triggered control issues have been addressed for uncertain lower-triangular nonlinear systems [22,23]. In [24–28], adaptive fuzzy or neural network event-triggered control methods were developed to compensate for non-parametric nonlinear uncertainties. However, in the event-triggered control field, the quantized state-feedback information of uncertain lower-triangular nonlinear systems has not been used to address the neural-network-based adaptive tracking problem thus far.

The aim of this paper is to establish a quantized-feedback-based event-triggered control methodology for the adaptive tracking of nonlinear strict-feedback systems with unknown nonlinearities and external disturbances. An approximation-based recursive control design using quantized state variables is developed to deal with unmatched and unknown nonlinearities and the time-varying disturbances. In the proposed design, adaptive laws and a triggering law using an auxiliary filter are derived by the quantized state variables. Furthermore, an adaptive tuning mechanism is provided to compensate for the effects of quantization and triggering errors. The stability of the closed-loop system and the prevention of Zeno behavior are analyzed in the Lyapunov sense.

Compared with existing related literature, the primary contributions of this paper are emphasized as follows:

(C1) Different from the recursive quantized feedback tracking method [14] where unmatched nonlinearities were known, the proposed tracking approach is capable of dealing with unmatched and unknown nonlinearities. This is achieved by designing quantized-states-based adaptive approximators and deriving three lemmas for the boundedness of the adaptation parameters and the quantization error signals.

(C2) The existing adaptive event-triggered control schemes [18,21–26,28] for nonlinear systems in a lower-triangular form did not consider the state quantization problem of nonlinear systems. In this paper, we first present a quantized-feedback-based event-triggered control strategy with a triggering law using quantized state variables. For this purpose, a triggering law using an auxiliary control input filter is designed to ensure the existence of inter-event time.

2. Problem Formulation

Consider a class of uncertain nonlinear systems in a strict-feedback form described by

$$\begin{aligned}\dot{x}_i &= x_{i+1} + f_i(\bar{x}_i) + d_i, \\ \dot{x}_n &= u + f_n(\bar{x}_n) + d_n,\end{aligned}\tag{1}$$

where $i = 1, \dots, n-1$, $\bar{x}_j = [x_1, \dots, x_j] \in \mathbb{R}^j$, $j = 1, \dots, n$, are state variable vectors, d_j are unknown time-varying disturbances satisfying $|d_j| \leq d_j^*$ with unknown constants $d_j^* > 0$, $u \in \mathbb{R}$ is the control

input, and $f_j(\cdot) : \mathbb{R}^j \mapsto \mathbb{R}$ are unknown C^1 nonlinear functions. In this paper, the control input u is an intermittently updated signal in time by an event-triggering law to be designed later. In addition, u is designed based on the quantized state variables obtained through the following uniform quantizer

$$q(x_i) = \begin{cases} \chi_l, & \chi_l - \frac{\delta}{2} \leq x_i < \chi_l + \frac{\delta}{2} \\ 0, & -\frac{\delta}{2} \leq x_i < \frac{\delta}{2} \\ -\chi_l, & -\chi_l - \frac{\delta}{2} \leq x_i < -\chi_l + \frac{\delta}{2} \end{cases} \quad (2)$$

where $i = 1, \dots, n, l \in \mathbb{Z}^+, \delta$ is the length of the quantization interval, $\chi_1 = \delta$, and $\chi_{l+1} = \chi_l + \delta$. Note that $q(x_i)$ is in a countable set $Q = \{0, \pm\chi_l\}$ and the quantization error $\kappa_{x,i} \triangleq x_i - x_i^q$ has the property $|\kappa_{x,i}| \leq \delta$ where $x_i^q \triangleq q(x_i)$ [17].

Assumption 1. Ref. [13] The quantized states $x_i^q, i = 1, \dots, n$, are available for feedback, instead of x_i .

Assumption 2. Ref. [5] The reference signal r and its time derivatives \dot{r} and \ddot{r} are bounded.

Lemma 1. Ref. [29] For any $\eta > 0$ and $v \in \mathbb{R}$, it is ensured that $0 \leq |v| - v \tanh(v/\eta) \leq 0.2785\eta$.

Lemma 2. Ref. [30] When a matrix $A \in \mathbb{R}^{n \times n}$ is Hurwitz, it is satisfied that $\|e^{At}\| \leq \beta_1 e^{-\beta_2 t}$ with $\beta_1 = \sqrt{\lambda_{\max}(G)/\lambda_{\min}(G)}$ and $\beta_2 = 1/\lambda_{\max}(G)$. Here, G is a symmetric positive definite matrix such that $A^T G + GA = -2I$ where I is an identity matrix of order n . In addition, $\lambda_{\max}(G)$ and $\lambda_{\min}(G)$ are the maximum and minimum eigenvalues of G , respectively.

Problem 1. Consider the uncertain strict-feedback nonlinear system (1) with unknown nonlinearities and state quantizer (2). Our control problem is to provide a quantized-feedback-based event-triggered tracking law u so that the state x_1 follows the reference signal r while all the closed-loop signals remain bounded.

Remark 1. Several real-world applications such as robot manipulations, electrical power systems, and aircraft systems can be modeled as system (1) [4,5]. Recent advances in the network technology enable the control of these systems over a network with limited communication resources. Then, the proposed theoretical result can be applied to these network-based practical control problems.

Remark 2. Compared with the existing control results reported in the related literature [13,14,21–26], this study considers both the quantized state feedback and the event-triggered control problems in the recursive control framework of nonlinear lower-triangular systems. Accordingly, Problem 1 cannot be resolved by using the approaches presented in [13,14,21–26].

3. Quantized-Feedback-Based Adaptive Event-Triggered Tracking

3.1. Radial Basis Function Neural Networks

According to the universal approximation property of radial basis function neural networks (RBFNNs) [31], if the number of neural nodes N is sufficiently large and the basis functions $s_i, i = 1, \dots, N$, are appropriately chosen, there exists an ideal bounded weight vector $W^* \in \mathbb{R}^N$, that satisfies $\|W^*\| \leq \check{W}$ with a constant \check{W} , such that

$$f(\varrho) = W^{*\top} S(\varrho) + \varepsilon(\varrho), \quad \varrho \in \Omega, \quad (3)$$

where $f(\varrho) : \Omega \mapsto \mathbb{R}$ is an unknown function; $\Omega \subset \mathbb{R}^M$ is a compact set, $\varrho = [\varrho_1, \dots, \varrho_M]^\top$ is an input vector with M elements, ε represents an approximation reconstruction error satisfying $|\varepsilon| \leq \varepsilon^*$ with a constant $\varepsilon^* > 0$, and $S(\varrho) = [s_1(\varrho), \dots, s_N(\varrho)]^\top \in \mathbb{R}^N$ is a basis function vector. In this study, $s_i(\varrho)$ are chosen as Gaussian functions $s_i(\varrho) = e^{-\|\varrho - c_i\|^2/\varphi^2}$ where $i = 1, \dots, N, c_i = [c_{i1}, \dots, c_{iM}]^\top \in \mathbb{R}^M$ is the

center of the receptive field and φ is the width of the Gaussian functions. Note that Gaussian basis function vector is bounded as $\|S(q)\| \leq S^*$ where S^* is a constant [32,33].

3.2. Quantized-Feedback-Based Event-Triggered Tracker Design

Based on the command filtered backstepping control technique [6], the proposed controller design procedure is conducted recursively. In this recursive design procedure, we use the following coordinate transformation

$$\begin{aligned} \mu_1 &= x_1 - r, \\ \mu_{j+1} &= x_{j+1} - \hat{\alpha}_{j,1}, \\ \tilde{\alpha}_{j,1} &= \hat{\alpha}_{j,1} - \alpha_j, \end{aligned} \tag{4}$$

where $j = 1, \dots, n - 1$, $\mu_i, i = 1, \dots, n$ are error surfaces, $\tilde{\alpha}_{j,1}$ are filtering errors, and α_j and $\hat{\alpha}_{j,1}$ are virtual control laws and their filtered signals, respectively. The signals $\hat{\alpha}_{j,1}$ are calculated from the following low-pass filters

$$\begin{aligned} \hat{\alpha}_{j,1} &= \hat{\alpha}_{j,2}, \\ \hat{\alpha}_{j,2} &= -2\zeta_j\omega_j\hat{\alpha}_{j,2} - \omega_j^2(\hat{\alpha}_{j,1} - \alpha_j), \end{aligned} \tag{5}$$

with $\hat{\alpha}_{j,1}(0) = \alpha_j(0)$ and $\hat{\alpha}_{j,2}(0) = 0$. $\zeta_j > 0$ and $\omega_j > 0$ are the damping factors and the natural frequencies, respectively.

Step 1: Consider the first error surface μ_1 . From (1) and (4), we have $\dot{\mu}_1 = x_2 + f_1 + d_1 - \dot{r} = \mu_2 + \tilde{\alpha}_{1,1} + \alpha_1 + f_1 + d_1 - \dot{r}$. Define a Lyapunov function candidate $V_1 = (1/2)\mu_1^2$. Then, employing an RBFNN to estimate the unknown function f_1 , the time derivative of V_1 is given by

$$\begin{aligned} \dot{V}_1 &= \mu_1(\mu_2 + \tilde{\alpha}_{1,1} + \alpha_1 + f_1 + d_1 - \dot{r}) \\ &= \mu_1(\mu_2 + \tilde{\alpha}_{1,1} + \alpha_1 + W_1^{*\top} S_1 + \varepsilon_1 + d_1 - \dot{r}), \end{aligned} \tag{6}$$

where W_1^* is an optimal weight, $S_1(x_1)$ denotes a basis function vector, and ε_1 is the reconstruction error for estimating f_1 .

The virtual control law α_1 is designed as

$$\alpha_1 = -k_1\mu_1 - \hat{W}_1^\top S_1 - \hat{b}_1 \tanh_1 + \dot{r}, \tag{7}$$

where $k_1 > 0$ is a control gain, \hat{W}_1 is the estimate of W_1^* , \hat{b}_1 are the estimate of an unknown constant b_1^* to be defined later, and $\tanh_1 = \tanh(\mu_1/\eta_1)$; $\eta_1 > 0$ is a design parameter.

Applying (7) into (6), we have

$$\begin{aligned} \dot{V}_1 &\leq \mu_1(\mu_2 + \tilde{\alpha}_{1,1}) - k_1\mu_1^2 - \mu_1\tilde{W}_1^\top S_1 - \mu_1\tilde{b}_1 \tanh_1 \\ &\quad - \mu_1b_1^* \tanh_1 + \mu_1(\varepsilon_1 + d_1), \end{aligned} \tag{8}$$

where $\tilde{W}_1 = \hat{W}_1 - W_1^*$ and $\tilde{b}_1 = \hat{b}_1 - b_1^*$ are estimation errors.

Step j ($j = 2, \dots, n - 1$): From (5), we have $\hat{\alpha}_{j,1} = \hat{\alpha}_{j,2}$. Thus, the time derivative of $V_j = (1/2)\mu_j^2$ is obtained as

$$\begin{aligned} \dot{V}_j &= \mu_j(\mu_{j+1} + \tilde{\alpha}_{j,1} + \alpha_j + f_j + d_j - \dot{\alpha}_{j-1,2}) \\ &= \mu_j(\mu_{j+1} + \tilde{\alpha}_{j,1} + \alpha_j + W_j^{*\top} S_j + \varepsilon_j + d_j - \dot{\alpha}_{j-1,2}), \end{aligned} \tag{9}$$

where W_j^* is an optimal weighting vector, $S_j(\bar{x}_j)$ is a basis function vector, and ε_j is the reconstruction error for approximating f_j .

Now, we choose the virtual control law α_j as follows:

$$\alpha_j = -k_j \mu_j - \hat{W}_j^\top S_j - \hat{b}_j \tanh_j + \hat{\alpha}_{j-1,2}, \tag{10}$$

where $k_j > 0$ is a control gain and \hat{W}_j is the estimate of W_j^* , and \hat{b}_j is the estimate of b_j^* to be defined later, and $\tanh_j = \tanh(\mu_j/\eta_j)$; $\eta_j > 0$ is a design parameter.

Substituting (10) into (9) yields that

$$\dot{V}_j \leq \mu_j(\mu_{j+1} + \tilde{\alpha}_{j,1}) - k_j \mu_j^2 - \mu_j \tilde{W}_j^\top S_j - \mu_j \tilde{b}_j \tanh_j - \mu_j b_j^* \tanh_j + \mu_j(\varepsilon_j + d_j) \tag{11}$$

where $\tilde{W}_j = \hat{W}_j - W_j^*$ and $\tilde{b}_j = \hat{b}_j - b_j^*$ are estimation errors.

Step n : Consider a Lyapunov function candidate $V_n = (1/2)\mu_n^2$. Similar to the previous steps, the time derivative of V_n satisfies

$$\dot{V}_n \leq \mu_n(u + W_n^{*\top} S_n + \varepsilon_n + d_n - \hat{\alpha}_{n-1,2}), \tag{12}$$

where W_n^* is an optimal weight, S_n is a basis function vector, and ε_n is the reconstruction error.

In order to design an actual control law u based on the quantized states, quantized-states-based error surfaces μ_i^q , virtual control laws α_j^q , and adaptation laws for \hat{W}_j and \hat{b}_j are defined as follows:

$$\begin{aligned} \mu_1^q &= x_1^q - r, \\ \mu_{j+1}^q &= x_{j+1}^q - \hat{\alpha}_{j,1}^q, \end{aligned} \tag{13}$$

$$\alpha_j^q = -k_j \mu_j^q - \hat{W}_j^\top S_j^q - \hat{b}_j \tanh_j^q + \hat{\alpha}_{j-1,2}^q, \tag{14}$$

$$\dot{\hat{W}}_j = \gamma_{w,j}(\mu_j^q S_j^q - \sigma_{w,j} |\mu_j^q| \hat{W}_j), \tag{15}$$

$$\dot{\hat{b}}_j = \gamma_{b,j}(\mu_j^q \tanh_j^q - \sigma_{b,j} |\mu_j^q| \hat{b}_j), \tag{16}$$

where $i = 1, \dots, n, j = 1, \dots, n - 1, S_j^q = S_j(\bar{x}_j^q)$; $\bar{x}_j^q = [x_1^q, \dots, x_j^q]^\top$, $\tanh_j^q = \tanh(\mu_j^q/\eta_j)$, and $\hat{\alpha}_{0,2}^q = \dot{r}$. $\gamma_{w,j} > 0$ are tuning gain matrices, $\gamma_{b,j} > 0$ are tuning gain constants, $\sigma_{w,j}$ and $\sigma_{b,j}$ are positive constants for σ -modification. The filtered signals $\hat{\alpha}_{j,1}^q$ and $\hat{\alpha}_{j,2}^q$ are obtained from the following filters

$$\begin{aligned} \dot{\hat{\alpha}}_{j,1}^q &= \hat{\alpha}_{j,2}^q, \\ \dot{\hat{\alpha}}_{j,2}^q &= -2\zeta_j \omega_j \hat{\alpha}_{j,2}^q - \omega_j^2 (\hat{\alpha}_{j,1}^q - \alpha_j^q), \end{aligned} \tag{17}$$

with $\hat{\alpha}_{j,1}^q(0) = \alpha_j^q(0)$ and $\hat{\alpha}_{j,2}^q(0) = 0$.

Then, a quantized-feedback-based adaptive event-triggered actual control law u with a triggering law is presented as

$$u(t) = \hat{\alpha}_{n,1}^q(t_l), \quad t \in [t_l, t_{l+1}), \tag{18}$$

$$t_{l+1} = \inf\{t \geq t_l \mid |u_e(t)| \geq \theta_1 |\mu_n^q(t)| + \theta_2\}, \tag{19}$$

$$\alpha_n^q = -k_n \mu_n^q - \hat{W}_n^\top S_n^q - \hat{b}_n \tanh_n^q + \hat{\alpha}_{n-1,2}^q, \tag{20}$$

$$\dot{\hat{W}}_n = \gamma_{w,n}(\mu_n^q S_n^q - \sigma_{w,n} |\mu_n^q| \hat{W}_n), \tag{21}$$

$$\dot{\hat{b}}_n = \gamma_{b,n}(\mu_n^q \tanh_n^q - \sigma_{b,n} |\mu_n^q| \hat{b}_n), \tag{22}$$

where $u_e(t) = u(t) - \hat{\alpha}_{n,1}^q(t)$, $l \in \mathbb{Z}^+$, $t_1 = 0$, t_l denotes the l th event time, $\theta_1, \theta_2 > 0$ are design parameters for the triggering law (19), \hat{W}_n is the estimate of W_n^* , and \hat{b}_n is the estimate of unknown constant b_n^* to be defined later, $\tanh_n^q = \tanh(\mu_n^q/\eta_n)$; $\eta_n > 0$ is a design constant, $S_n^q = S_n(\bar{x}_n^q)$;

$\bar{x}_n^q = [x_1^q, \dots, x_n^q]^T$, $k_n > 0$ is a control gain, $\gamma_{w,n} > 0$ and $\gamma_{b,n} > 0$ are tuning gains, and $\sigma_{w,n} > 0$ and $\sigma_{b,n} > 0$ are small constants for σ -modification. Here, $\hat{\alpha}_{n,1}^q$ in u_e is a filtered signal of α_n^q given by

$$\begin{aligned} \hat{\alpha}_{n,1}^q &= \hat{\alpha}_{n,2}^q, \\ \dot{\hat{\alpha}}_{n,2}^q &= -2\zeta_n\omega_n\hat{\alpha}_{n,2}^q - \omega_n^2(\hat{\alpha}_{n,1}^q - \alpha_n^q), \end{aligned} \tag{23}$$

where ω_n and ζ_n are filter design parameters, $\hat{\alpha}_{n,1}^q(0) = \alpha_n^q(0)$, and $\hat{\alpha}_{n,2}^q(0) = 0$. Note that the actual input u is fixed as a constant value $\hat{\alpha}_{n,1}^q(t_l)$ until the next event occurs at t_{l+1} and each event time is determined by checking the condition in (19). The block diagram of the proposed control scheme consisting of (14)–(23) is shown in Figure 1.

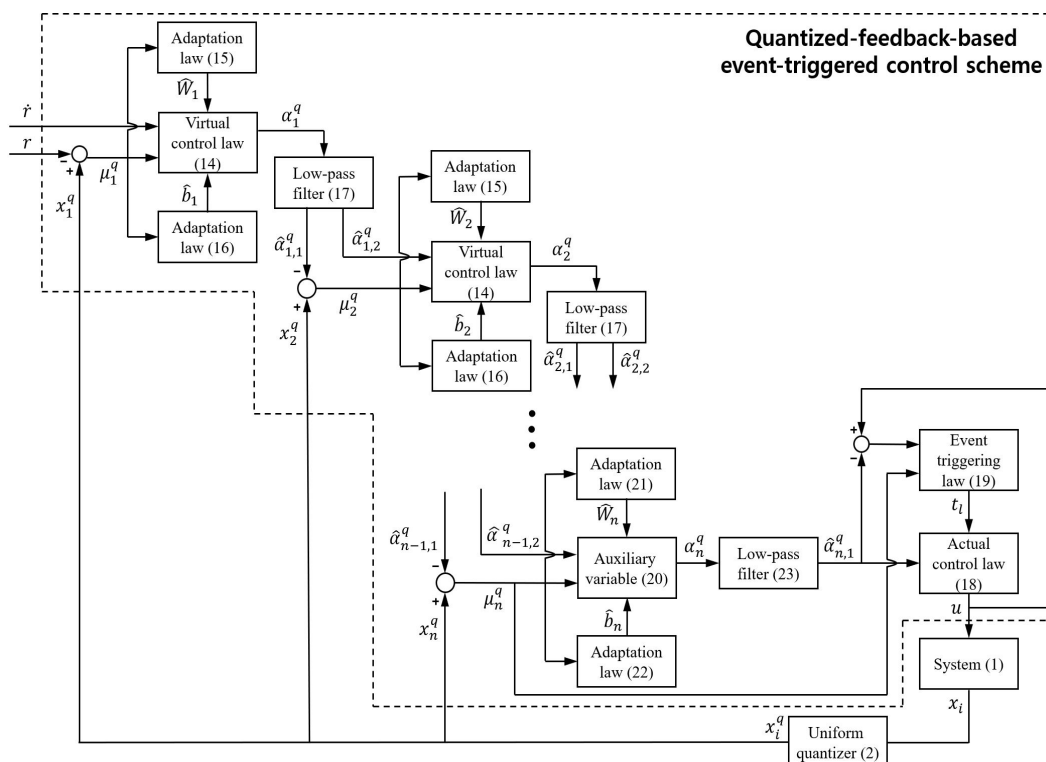


Figure 1. Block diagram of the proposed quantized-feedback-based event-triggered tracking system.

Define an ideal control signal α_n as

$$\alpha_n = -k_n\mu_n - \hat{W}_n^T S_n - \hat{b}_n \tanh_n + \hat{\alpha}_{n-1,2} \tag{24}$$

and its filtered signals $\hat{\alpha}_{n,1}$ and $\hat{\alpha}_{n,2}$ obtained from the following filter

$$\begin{aligned} \hat{\alpha}_{n,1} &= \hat{\alpha}_{n,2}, \\ \dot{\hat{\alpha}}_{n,2} &= -2\zeta_n\omega_n\hat{\alpha}_{n,2} - \omega_n^2(\hat{\alpha}_{n,1} - \alpha_n) \end{aligned} \tag{25}$$

where $\hat{\alpha}_{n,1}(0) = \alpha_n(0)$ and $\hat{\alpha}_{n,2}(0) = 0$.

Note that the following property holds.

$$u + \alpha_n - \alpha_n + \hat{\alpha}_{n,1} - \hat{\alpha}_{n,1} + \hat{\alpha}_{n,1}^q - \hat{\alpha}_{n,1}^q = u_e + \alpha_n + \tilde{\alpha}_{n,1} - \kappa_{\hat{\alpha}_{n,1}}, \tag{26}$$

where $\tilde{\alpha}_{n,1} = \hat{\alpha}_{n,1} - \alpha_n$ and $\kappa_{\hat{\alpha}_{n,1}} = \hat{\alpha}_{n,1} - \hat{\alpha}_{n,1}^q$.

By substituting (26) into (12) and using (24), we have

$$\dot{V}_n \leq \mu_n(\alpha_n + W_n^{*T} S_n + \varepsilon_n + d_n - \hat{\alpha}_{n-1,2}) + \mu_n(\tilde{\alpha}_{n,1} - \kappa_{\hat{\alpha}_{n,1}}) + \mu_n u_e$$

$$\begin{aligned}
 &= -k_n \mu_n^2 - \mu_n \tilde{W}_n^\top S_n - \mu_n \tilde{b}_n \tanh_n + \mu_n (\tilde{\alpha}_{n,1} - \kappa_{\hat{\alpha},n,1}) + \mu_n u_e \\
 &\quad - \mu_n \tilde{b}_n^* \tanh_n + \mu_n (\varepsilon_n + d_n)
 \end{aligned}
 \tag{27}$$

where $\tilde{W}_n = \hat{W}_n - W_n^*$ and $\tilde{b}_n = \hat{b}_n - b_n^*$ are estimation errors.

Remark 3. In the proposed triggering law (19), the adaptive terms depend on the time-varying error surface $\mu_n^q = x_n^q - \hat{\alpha}_{n-1,1}^q$. Note that $\hat{\alpha}_{n-1,1}^q$ is the filtered signal of α_{n-1}^q from (14) and α_{n-1}^q includes the adaptation parameters \hat{W}_{n-1} and \hat{b}_{n-1} and the error surface μ_{n-2}^q . A similar reasoning can apply the error surface μ_{n-2}^q recursively. In addition, α_n^q obtained from (20) is employed in u_e of (19). Therefore, it concludes that the triggering law (19) depends on the information of all adaptation parameters \hat{W}_i and \hat{b}_i where $i = 1, \dots, n$.

3.3. Stability Analysis

Let us define $\tilde{\alpha}_{i,2} = \hat{\alpha}_{i,2}$ and $\tilde{\alpha}_i = [\tilde{\alpha}_{i,1}, \tilde{\alpha}_{i,2}]^\top$, $\tilde{r} = [r, \dot{r}, \ddot{r}]^\top$, $\tilde{\mu}_i = [\mu_1, \dots, \mu_i]^\top$, $\tilde{\alpha}_{i,1} = [\tilde{\alpha}_{1,1}, \dots, \tilde{\alpha}_{i,1}]^\top$, $\tilde{\alpha}_{i,2} = [\tilde{\alpha}_{1,2}, \dots, \tilde{\alpha}_{i,2}]^\top$, $\tilde{W}_i = [\hat{W}_1, \dots, \hat{W}_i]^\top$, $\tilde{b}_i = [\hat{b}_1, \dots, \hat{b}_i]^\top$, and $\tilde{d}_i = [d_1, \dots, d_i]^\top$ for $i = 1, \dots, n$. Then, the dynamics of $\tilde{\alpha}_i$ along (5) and (25) is given by

$$\dot{\tilde{\alpha}}_i = A_i \tilde{\alpha}_i + D \Gamma_i,
 \tag{28}$$

where $A_i = \begin{bmatrix} 0 & 1 \\ -\omega_i^2 & -2\zeta_i \omega_i \end{bmatrix}$, $D = [1, 0]^\top$, and

$$\begin{aligned}
 \Gamma_1(\tilde{\mu}_2, \tilde{\alpha}_{1,1}, \hat{W}_1, \hat{b}_1, \tilde{r}, d_1) &= k_1 \dot{\mu}_1 + \hat{W}_1^\top S_1 + \hat{W}_1^\top \dot{S}_1 + \hat{b}_1 \tanh_1 + \hat{b}_1 \operatorname{sech}^2\left(\frac{\mu_1}{\eta_1}\right) \frac{\dot{\mu}_1}{\eta_1} - \ddot{r}, \\
 \Gamma_j(\tilde{\mu}_{j+1}, \tilde{\alpha}_{j,1}, \tilde{\alpha}_{j-1,2}, \tilde{W}_j, \tilde{b}_j, \tilde{r}, \tilde{d}_j) &= k_j \dot{\mu}_j + \hat{W}_j^\top S_j + \hat{W}_j^\top \dot{S}_j + \hat{b}_j \tanh_j + \hat{b}_j \operatorname{sech}^2\left(\frac{\mu_j}{\eta_j}\right) \frac{\dot{\mu}_j}{\eta_j} - \dot{\tilde{\alpha}}_{j-1,2}, \\
 \Gamma_n(\tilde{\mu}_n, \tilde{\alpha}_{n,1}, \tilde{\alpha}_{n-1,2}, \tilde{W}_n, \tilde{b}_n, \tilde{r}, \tilde{d}_n, u_e, \kappa_{\hat{\alpha},n,1}) &= k_n \dot{\mu}_n + \hat{W}_n^\top S_n + \hat{W}_n^\top \dot{S}_n + \hat{b}_n \tanh_n \\
 &\quad + \hat{b}_n \operatorname{sech}^2\left(\frac{\mu_n}{\eta_n}\right) \frac{\dot{\mu}_n}{\eta_n} - \dot{\tilde{\alpha}}_{n-1,2},
 \end{aligned}
 \tag{29}$$

for $j = 2, \dots, n - 1$.

Owing to $\zeta_i > 0$ and $\omega_i > 0$, A_i are Hurwitz matrices. Then, for any matrix $M_i > 0$, $A_i^\top P_i + P_i A_i = -M_i$ is satisfied where $P_i > 0$ is a symmetric matrix.

For the stability analysis of the closed-loop system, three lemmas (i.e., Lemmas 3–5) are presented. Lemmas 3 and 4 give the boundedness of the estimation errors \tilde{W}_i and \tilde{b}_i , respectively, where $i = 1, \dots, n$. In Lemma 5, we show that the errors between the quantized signals μ_i^q , S_i^q , \tanh_i^q , α_i^q , $\hat{\alpha}_{i,1}^q$, and $\hat{\alpha}_{i,2}^q$ and the unquantized signals μ_i , S_i , \tanh_i , α_i , $\hat{\alpha}_{i,1}$, and $\hat{\alpha}_{i,2}$ are bounded where $i = 1, \dots, n$.

Lemma 3. Consider the adaptation laws (15) and (21). Then, there exists a compact set $\Omega_{w,i} = \{\tilde{W}_i \mid \|\tilde{W}_i\| \leq \chi_{w,i}\}$ such that $\tilde{W}_i(t) \in \Omega_{w,i}$ for all $t \geq 0$ provided that $\tilde{W}_i(0) \in \Omega_{w,i}$ where $\chi_{w,i}$ is an unknown constant.

Proof. Let us consider a Lyapunov function candidate $V_{w,i} = (1/2) \tilde{W}_i^\top \gamma_{w,i}^{-1} \tilde{W}_i$. Then, $\dot{V}_{w,i}$ is given by

$$\begin{aligned}
 \dot{V}_{w,i} &= \tilde{W}_i^\top (\mu_i^q S_i^q - \sigma_{w,i} |\mu_i^q| \tilde{W}_i) \\
 &= \tilde{W}_i^\top (\mu_i^q S_i^q - \sigma_{w,i} |\mu_i^q| (W_i^* + \tilde{W}_i)).
 \end{aligned}$$

Here, each term can be represented by $-\sigma_{w,i} |\mu_i^q| \tilde{W}_i^\top \tilde{W}_i = -\sigma_{w,i} |\mu_i^q| \|\tilde{W}_i\|^2$, $\tilde{W}_i^\top \mu_i^q S_i^q \leq \|\tilde{W}_i\| |\mu_i^q| \|S_i^q\|$, and $-\tilde{W}_i^\top \sigma_{w,i} |\mu_i^q| W_i^* \leq \|\tilde{W}_i\| |\mu_i^q| \sigma_{w,i} \|W_i^*\|$. Here, since the optimal weights W_i^* and the basis function vectors S_i are bounded, there exist constants \tilde{W}_i^* and S_i^* satisfying $\|W_i^*\| \leq \tilde{W}_i^*$ and $\|S_i^q\| \leq S_i^*$, respectively. Based on these facts, $\dot{V}_{w,i}$ satisfies

$$\dot{V}_{w,i} \leq \|\tilde{W}_i\| |\mu_i^q| (S_i^* + \sigma_{w,i} \tilde{W}_i^* - \sigma_{w,i} \|\tilde{W}_i\|).
 \tag{30}$$

From this inequality, we have that $\dot{V}_{w,i} \leq 0$ when $\|\tilde{W}_i\| \geq \chi_{w,i}$ with $\chi_{w,i} \triangleq (S_i^* + \sigma_{w,i}\tilde{W}_i)/\sigma_{w,i}$. Thus, $V_{w,i}$ decreases when $\tilde{W}_i(t) \notin \Omega_{w,i}$ and \tilde{W}_i finally remains within $\Omega_{w,i}$. Consequently, if $\tilde{W}_i(0) \in \Omega_{w,i}$, $\tilde{W}_i(t) \in \Omega_{w,i}$ for all $t \geq 0$ which completes the proof. \square

Lemma 4. Consider the adaptation laws (16) and (22). Then, there exists a compact set $\Omega_{b,i} = \{\tilde{b}_i \mid |\tilde{b}_i| \leq \chi_{b,i}\}$ such that $\tilde{b}_i(t) \in \Omega_{b,i}$ for all $t \geq 0$ provided that $\tilde{b}_i(0) \in \Omega_{b,i}$ where $\chi_{b,i}$ is an unknown constant.

Proof. Similar to the proof of Lemma 3, a Lyapunov function candidate $V_{b,i} = (1/(2\gamma_{b,i}))\tilde{b}_i^2$ is considered. Then, we have

$$\begin{aligned} \dot{V}_{b,i} &= \tilde{b}_i(\mu_i^q \tanh_i^q - \sigma_{b,i}|\mu_i^q|\hat{b}_i) \\ &= \tilde{b}_i(\mu_i^q \tanh_i^q - \sigma_{b,i}|\mu_i^q|(b_i^* + \tilde{b}_i)). \end{aligned}$$

Using $b_i^* > 0$ and the inequality $|\tanh_i^q| \leq 1$, it is obtained that $\tilde{b}_i\mu_i^q \tanh_i^q \leq |\tilde{b}_i||\mu_i^q|$, $-\tilde{b}_i\sigma_{b,i}|\mu_i^q|b_i^* \leq |\tilde{b}_i||\mu_i^q|\sigma_{b,i}b_i^*$, and $-\tilde{b}_i^2\sigma_{b,i}|\mu_i^q| = -|\tilde{b}_i||\mu_i^q|\sigma_{b,i}|\tilde{b}_i|$. Then, $\dot{V}_{b,i}$ becomes

$$\dot{V}_{b,i} \leq |\tilde{b}_i||\mu_i^q|(1 + \sigma_{b,i}b_i^* - \sigma_{b,i}|\tilde{b}_i|). \tag{31}$$

Let $\chi_{b,i} \triangleq (1 + \sigma_{b,i}b_i^*)/\sigma_{b,i}$. Then, following an argument similar to that in the proof of Lemma 3, it is ensured that if $\tilde{b}_i(0) \in \Omega_{b,i}$, $\tilde{b}_i(t) \in \Omega_{b,i}$ for all $t \geq 0$ which completes the proof. \square

Lemma 5. Consider the quantization errors of the closed-loop signals as

$$\begin{aligned} \kappa_{\mu,i} &= \mu_i - \mu_i^q, & \kappa_{S,i} &= S_i - S_i^q, \\ \kappa_{\text{th},i} &= \tanh_i - \tanh_i^q, & \kappa_{\alpha,i} &= \alpha_i - \alpha_i^q, \\ \kappa_{\hat{\alpha},i,1} &= \hat{\alpha}_{i,1} - \hat{\alpha}_{i,1}^q, & \kappa_{\hat{\alpha},i,2} &= \hat{\alpha}_{i,2} - \hat{\alpha}_{i,2}^q, \end{aligned} \tag{32}$$

where $i = 1, \dots, n$. Then, there exist positive constants $K_{\mu,i}$, $K_{S,i}$, $K_{\text{th},i}$, $K_{\alpha,i}$, and $K_{\hat{\alpha},i}$ such that $|\kappa_{\mu,i}| \leq K_{\mu,i}$, $\|\kappa_{S,i}\| \leq K_{S,i}$, $|\kappa_{\text{th},i}| \leq K_{\text{th},i}$, $|\kappa_{\alpha,i}| \leq K_{\alpha,i}$, and $\|\kappa_{\hat{\alpha},i}\| \leq K_{\hat{\alpha},i}$, respectively, where $\kappa_{\hat{\alpha},i} = [\kappa_{\hat{\alpha},i,1}, \kappa_{\hat{\alpha},i,2}]^\top$.

Proof. (i) Based on the boundedness of Gaussian basis functions and hyperbolic tangent functions, we can easily obtain

$$\|\kappa_{S,i}\| \leq K_{S,i}, \quad |\kappa_{\text{th},i}| \leq K_{\text{th},i}, \tag{33}$$

where $K_{S,i} = 2S_i^*$ and $K_{\text{th},i} = 2$. Using the property $|\kappa_{x,i}| \leq \delta$ of the uniform quantizer (2) and $\kappa_{\mu,1} = x_1 - x_1^q$, $\kappa_{\mu,1}$ satisfies

$$|\kappa_{\mu,1}| = |\kappa_{x,1}| \leq K_{\mu,1} \tag{34}$$

where $K_{\mu,1} = \delta$. From (7) and (14), we have

$$\kappa_{\alpha,1} = -k_1\kappa_{\mu,1} - \hat{W}_1^\top \kappa_{S,1} - \hat{b}_1\kappa_{\text{th},1}.$$

Then, it holds that

$$|\kappa_{\alpha,1}| \leq k_1|\kappa_{\mu,1}| + \|\hat{W}_1\|\|\kappa_{S,1}\| + |\hat{b}_1||\kappa_{\text{th},1}|. \tag{35}$$

From Lemmas 3 and 4, we have $\|\tilde{W}_i\| \leq \chi_{w,i}^*$ and $|\tilde{b}_i| \leq \chi_{b,i}^*$ where $\chi_{w,i}^* = \max\{\|\tilde{W}_i(0)\|, \chi_{w,i}\}$ and $\chi_{b,i}^* = \max\{|\tilde{b}_i(0)|, \chi_{b,i}\}$. Then, using $\hat{W}_1 = \tilde{W}_1 + W_1^*$ and $\hat{b}_1 = \tilde{b}_1 + b_1^*$, the bounding constant $K_{\alpha,1}$ is obtained as $K_{\alpha,1} \triangleq k_1K_{\mu,1} + (\chi_{w,1}^* + \tilde{W}_1)K_{S,1} + (\chi_{b,1}^* + b_1^*)K_{\text{th},1}$.

The low-pass filters for α_1 in (5) and for α_1^q in (17) induce

$$\dot{\kappa}_{\hat{\alpha},1} = A_1 \kappa_{\hat{\alpha},1} + \bar{D}_1 \kappa_{\alpha,1} \tag{36}$$

where $\kappa_{\hat{\alpha},1} = [\kappa_{\hat{\alpha},1,1}, \kappa_{\hat{\alpha},1,2}]^\top$ and $\bar{D}_1 = [0, \omega_1^2]$. Solving this differential equation leads to

$$\kappa_{\hat{\alpha},1}(t) = e^{A_1 t} \kappa_{\hat{\alpha},1}(0) + \int_0^t e^{A_1(t-\tau)} \bar{D}_1 \kappa_{\alpha,1}(\tau) d\tau. \tag{37}$$

Since A_1 is invertible, the following inequality is satisfied.

$$\|\kappa_{\hat{\alpha},1}(t)\| \leq \|e^{A_1 t}\| \|\kappa_{\hat{\alpha},1}(0)\| + K_{\alpha,1} \|\bar{D}_1\| \|A_1^{-1}\| \|I - e^{A_1 t}\|. \tag{38}$$

From Lemma 2, the inequality $\|e^{A_1 t}\| \leq \beta_{1,1} e^{-\beta_{1,2} t}$ holds with positive constants $\beta_{1,1}$ and $\beta_{1,2}$. Due to $\kappa_{\hat{\alpha},1,1}(0) = \kappa_{\alpha,1}(0)$ and $\kappa_{\hat{\alpha},1,2}(0) = 0$, we have $\|\kappa_{\hat{\alpha},1}(0)\| = |\kappa_{\alpha,1}(0)|$. Then, we have

$$\begin{aligned} \|\kappa_{\hat{\alpha},1}(t)\| &\leq \beta_{1,1} |\kappa_{\alpha,1}(0)| + K_{\alpha,1} \|\bar{D}_1\| \|A_1^{-1}\| (1 + \beta_{1,1}) \\ &\triangleq K_{\hat{\alpha},1}. \end{aligned} \tag{39}$$

Thus, it is guaranteed that $|\kappa_{\hat{\alpha},1,1}| \leq K_{\hat{\alpha},1}$ and $|\kappa_{\hat{\alpha},1,2}| \leq K_{\hat{\alpha},1}$.

(ii) From $\mu_2 = x_2 - \hat{\alpha}_{1,1}$ and $\mu_2^q = x_2^q - \hat{\alpha}_{1,1}^q$, it holds that

$$|\kappa_{\mu,2}| \leq |\kappa_{x,2}| + |\kappa_{\hat{\alpha},1,1}| \leq K_{\mu,2} \tag{40}$$

where $K_{\mu,2} \triangleq K_{x,2} + K_{\hat{\alpha},1}$; $K_{x,2} = \delta$ owing to the property $|\kappa_{x,i}| \leq \delta$. From (10) and (14), we have $\kappa_{\alpha,2} = -k_2 \kappa_{\mu,2} - \hat{W}_2^\top \kappa_{S,2} - \hat{b}_2 \kappa_{th,2} + \kappa_{\hat{\alpha},1,2}$. Then, it holds that

$$|\kappa_{\alpha,2}| \leq k_2 |\kappa_{\mu,2}| + \|\hat{W}_2\| \|\kappa_{S,2}\| + |\hat{b}_2| |\kappa_{th,1}| + |\kappa_{\hat{\alpha},1,2}| \leq K_{\alpha,2} \tag{41}$$

where $K_{\alpha,2} \triangleq k_2 K_{\mu,2} + (\chi_{w,2}^* + \hat{W}_2) K_{S,2} + (\chi_{b,2}^* + \hat{b}_2) K_{th,2} + K_{\hat{\alpha},1}$. Following a procedure similar to that from (36)–(39), we can obtain the constant $K_{\hat{\alpha},2}$ satisfying $\|\kappa_{\hat{\alpha},2}\| \leq K_{\hat{\alpha},2}$.

(iii) According to the similar recursive derivation procedure, it holds that $\kappa_{\mu,i}$, $\kappa_{\alpha,i}$, and $\kappa_{\hat{\alpha},i}$, $i = 3, \dots, n$, are bounded as

$$|\kappa_{\mu,i}| \leq K_{\mu,i}, \quad |\kappa_{\alpha,i}| \leq K_{\alpha,i}, \quad \|\kappa_{\hat{\alpha},i}\| \leq K_{\hat{\alpha},i}.$$

This completes the proof of Lemma 5. \square

Choose a Lyapunov function candidate V as

$$V = \sum_{j=1}^n \left(V_j + \tilde{\alpha}_j^\top P_j \tilde{\alpha}_j \right). \tag{42}$$

Theorem 1. Consider the uncertain strict-feedback nonlinear system (1) with the uniform state quantizer (2). Then, for any initial conditions satisfying $V(0) \leq \varsigma$, the quantized-feedback-based adaptive event-triggered tracker consisting of the command filters (17) and (23), the virtual control laws (14), the actual event-triggered control law (18)–(20) with the adaptation laws (15), (16), (21) and (22) ensures that all the closed-loop signals are uniformly ultimately bounded, the tracking error μ_1 converges to an adjustable compact set around zero, and the inter-event times $t_{l+1} - t_l$ are lower bounded by the minimum inter-event time $t_{\min} > 0$ where $l \in \mathbb{Z}^+$.

Proof. From (8), (11), (27) and (29), \dot{V} is given by

$$\begin{aligned} \dot{V} \leq & - \sum_{j=1}^n k_j \mu_j^2 - \sum_{j=1}^n \tilde{\alpha}_j^\top M_j \tilde{\alpha}_j + \sum_{j=1}^{n-1} \mu_j \mu_{j+1} + \sum_{j=1}^n \mu_j \tilde{\alpha}_{j,1} + \sum_{j=1}^n 2\tilde{\alpha}_j^\top P_j D \Gamma_j \\ & - \sum_{j=1}^n \mu_j b_j^* \tanh_j + \sum_{j=1}^n \mu_j (\varepsilon_j + d_j - \tilde{W}_j^\top S_j) + \mu_n u_e - \mu_n \kappa_{\hat{\alpha},n,1} - \sum_{j=1}^n \mu_j \tilde{b}_j \tanh_j. \end{aligned} \tag{43}$$

From (19), the inequality

$$\begin{aligned} |\mu_n u_e| & \leq |\mu_n| (\theta_1 |\mu_n^q| + \theta_2) \\ & \leq \theta_1 \mu_n^2 + \theta_1 |\mu_n| |\mu_n^q - \mu_n| + \theta_2 |\mu_n| \end{aligned} \tag{44}$$

holds for all $t \geq 0$. From (44) and $\kappa_{\mu,n} = \mu_n - \mu_n^q$, we get

$$\begin{aligned} \dot{V} \leq & - \sum_{j=1}^{n-1} k_j \mu_j^2 - (k_n - \theta_1) \mu_n^2 - \sum_{j=1}^n \tilde{\alpha}_j^\top M_j \tilde{\alpha}_j + \sum_{j=1}^{n-1} \mu_j \mu_{j+1} + \sum_{j=1}^n \mu_j \tilde{\alpha}_{j,1} + \sum_{j=1}^n 2\tilde{\alpha}_j^\top P_j D \Gamma_j \\ & - \sum_{j=1}^n \mu_j b_j^* \tanh_j + \sum_{j=1}^n \mu_j b_j - \sum_{j=1}^n \mu_j \tilde{b}_j \tanh_j \end{aligned} \tag{45}$$

where $b_j = \varepsilon_j + d_j - \tilde{W}_j^\top S_j, j = 1, \dots, n - 1$, and $b_n = \varepsilon_n + d_n - \tilde{W}_n^\top S_n + \theta_1 |\kappa_{\mu,n}| \text{sgn}(\mu_n) + \theta_2 \text{sgn}(\mu_n) - \kappa_{\hat{\alpha},n,1}$; $\text{sgn}(\mu_n)$ denotes the signum function of μ_n .

The reconstruction errors ε_i , basis function vectors S_i , and time-varying disturbances d_i are bounded signals where $i = 1, \dots, n$. In addition, $\|\tilde{W}_i\|, i = 1, \dots, n$, are bounded from Lemma 3 and $\kappa_{\mu,n}$ and $\kappa_{\hat{\alpha},n,1}$ are bounded from Lemma 5. Therefore, b_j and b_n are bounded as

$$\begin{aligned} |b_j| & \leq \varepsilon_j^* + d_j^* + \chi_{w,j}^* S_j^* \triangleq b_j^*, \\ |b_n| & \leq \varepsilon_n^* + d_n^* + \chi_{w,n}^* S_n^* + \theta_1 K_{\mu,n} + \theta_2 + K_{\hat{\alpha},n} \triangleq b_n^*. \end{aligned}$$

Then, using the boundedness of $b_j, j = 1, \dots, n$, and applying Lemma 1, it holds that

$$|\mu_j b_j| \leq b_j^* |\mu_j| \leq b_j^* \mu_j \tanh_j + 0.2785 b_j^* \eta_j. \tag{46}$$

Using (46) yields

$$\begin{aligned} \dot{V} \leq & - \sum_{j=1}^{n-1} k_j \mu_j^2 - (k_n - \theta_1) \mu_n^2 - m_j \sum_{j=1}^n \|\tilde{\alpha}_j\|^2 + \sum_{j=1}^{n-1} \mu_j \mu_{j+1} + \sum_{j=1}^n \mu_j \tilde{\alpha}_{j,1} + \sum_{j=1}^n 2\tilde{\alpha}_j^\top P_j D \Gamma_j \\ & - \sum_{j=1}^n \mu_j \tilde{b}_j \tanh_j + \sum_{j=1}^n 0.2785 b_j^* \eta_j \end{aligned}$$

where $m_j = \lambda_{\min}(M_j)$.

From $|\kappa_{\mu,n}| \leq K_{\mu,n}$, we get $|u_e| \leq \theta_1 |\mu_n^q| + \theta_2 \leq \theta_1 |\mu_n| + \theta_1 K_{\mu,n} + \theta_2$. Then, since $\|\tilde{W}_i\| \leq \chi_{w,i}^*, |\tilde{b}_i| \leq \chi_{b,i}^*, |d_i| \leq d_i^*$, and $|\kappa_{\hat{\alpha},n,1}| \leq K_{\hat{\alpha},n}$ are satisfied for $i = 1, \dots, n$, there exist positive bounding functions Γ_i^* such that

$$\begin{aligned} |\Gamma_1(\bar{\mu}_2, \tilde{\alpha}_{1,1}, \hat{W}_1, \hat{b}_1, \bar{r}, d_1)| & \leq \Gamma_1^*(\bar{\mu}_2, \tilde{\alpha}_{1,1}, \bar{r}), \\ |\Gamma_j(\bar{\mu}_{j+1}, \tilde{\alpha}_{j,1}, \tilde{\alpha}_{j-1,2}, \tilde{W}_j, \tilde{b}_j, \bar{r}, \bar{d}_j)| & \leq \Gamma_j^*(\bar{\mu}_{j+1}, \tilde{\alpha}_{j,1}, \tilde{\alpha}_{j-1,2}, \bar{r}), \\ |\Gamma_n(\bar{\mu}_n, \tilde{\alpha}_{n,1}, \tilde{\alpha}_{n-1,2}, \tilde{W}_n, \tilde{b}_n, \bar{r}, \bar{d}_n, u_e, \kappa_{\hat{\alpha},n,1})| & \leq \Gamma_n^*(\bar{\mu}_n, \tilde{\alpha}_{n,1}, \tilde{\alpha}_{n-1,2}, \bar{r}), \end{aligned} \tag{47}$$

where $j = 2, \dots, n - 1$.

Let us define $\Xi_j, j = 1, \dots, n - 1, \Xi_n,$ and Ξ_r as $\Xi_j = \{(\mu_1, \dots, \mu_{j+1}, \tilde{\alpha}_1, \dots, \tilde{\alpha}_j) : \sum_{\rho=1}^{j+1} \mu_\rho^2 + \sum_{\rho=1}^j 2\tilde{\alpha}_\rho^\top P_\rho \tilde{\alpha}_\rho \leq 2\zeta\}, \Xi_n = \{(\mu_1, \dots, \mu_n, \tilde{\alpha}_1, \dots, \tilde{\alpha}_n) : \sum_{\rho=1}^n \mu_\rho^2 + \sum_{\rho=1}^n 2\tilde{\alpha}_\rho^\top P_\rho \tilde{\alpha}_\rho \leq 2\zeta\},$ and $\Xi_r = \{(r, \dot{r}, \ddot{r}) : r^2 + \dot{r}^2 + \ddot{r}^2 \leq \zeta_r\}$ where $\tilde{\alpha}_\rho = [\tilde{\alpha}_{\rho,1}, \tilde{\alpha}_{\rho,2}]^\top$ and $\zeta_r > 0$ is a constant. Note that $\Xi_j \in \mathbb{R}^{3j+1}, \Xi_n \in \mathbb{R}^{3n},$ and $\Xi_r \in \mathbb{R}^3$ are compact sets. Therefore, $\Xi_j \times \Xi_r \in \mathbb{R}^{3j+4}$ and $\Xi_n \times \Xi_r \in \mathbb{R}^{3n+3}$ are also compact. From (47), it is ensured that there exist constants $\bar{\Gamma}_j$ and $\bar{\Gamma}_n$ such that $|\Gamma_j^*| \leq \bar{\Gamma}_j$ on $\Xi_j \times \Xi_r$ and $|\Gamma_n^*| \leq \bar{\Gamma}_n$ on $\Xi_n \times \Xi_r$. Then, using the following inequalities

$$\begin{aligned} \mu_j \mu_{j+1} &\leq \frac{1}{2} \mu_j^2 + \frac{1}{2} \mu_{j+1}^2, \\ \mu_j \tilde{\alpha}_{j,1} &\leq \frac{1}{2} \mu_j^2 + \frac{1}{2} \|\tilde{\alpha}_j\|^2, \\ 2\tilde{\alpha}_j^\top P_j D \Gamma_j &\leq \frac{(\Gamma_j^*)^2 \|P_j\|^2 \|\tilde{\alpha}_j\|^2}{\iota} + \iota, \\ -\mu_j \tilde{b}_j \tanh_j &\leq \frac{1}{2} \mu_j^2 + \frac{1}{2} (\chi_{b,j}^*)^2, \end{aligned}$$

with a constant $\iota > 0,$ and selecting $k_1 = 3/2 + \bar{k}_1, k_j = 2 + \bar{k}_j, k_n = 3/2 + \theta_1 + \bar{k}_n, m_j = 1/2 + \bar{\Gamma}_j^2 \|P_j\|^2 / \iota + \bar{m}_j$ with positive constants $\bar{k}_1, \bar{k}_j, \bar{k}_n,$ and $\bar{m}_j,$ we get

$$\dot{V} \leq -\sum_{j=1}^n \bar{k}_j \mu_j^2 - \sum_{j=1}^n \bar{m}_j \|\tilde{\alpha}_j\|^2 - \sum_{j=1}^n \left(1 - \frac{(\Gamma_j^*)^2}{\bar{\Gamma}_j^2}\right) \frac{\bar{\Gamma}_j^2 \|P_j\|^2 \|\tilde{\alpha}_j\|^2}{\iota} + C \tag{48}$$

where $C = \sum_{j=1}^n 0.2785 b_j^* \eta_j + \sum_{j=1}^n (\chi_{b,j}^*)^2 + n\iota.$ Since $|\Gamma_j^*| \leq \bar{\Gamma}_j$ on $V = \varepsilon,$ it is obtained that $\dot{V} \leq -kV + C$ where $k = \min[2\bar{k}_1, \dots, 2\bar{k}_n, \bar{m}_1 / \lambda_{\max}(P_1), \dots, \bar{m}_n / \lambda_{\max}(P_n)].$ Here, when $k > C/\zeta, \dot{V} < 0$ on $V = \zeta$ is ensured and thus the set $V \leq \zeta$ is an invariant set. Therefore, we can conclude that the closed-loop signals μ_i and $\tilde{\alpha}_i$ are bounded where $i = 1, \dots, n.$ From the boundedness of μ_1 and r, x_1 is bounded. Then, α_1 in (7) is bounded using the boundedness of \hat{W}_1 and \hat{b}_1 from Lemmas 3 and 4. Based on the boundedness of $\alpha_1,$ it is induced that $\hat{\alpha}_{1,1}$ and $\hat{\alpha}_{1,2}$ are bounded owing to the stable filter (5). Thus, the boundedness of μ_2 and $\hat{\alpha}_{1,1}$ leads to the boundedness of $x_2.$ By the similar reasoning, $x_i, \alpha_i, \hat{\alpha}_{i,1},$ and $\hat{\alpha}_{i,2}$ are bounded for $i = 1, \dots, n.$ Then, from Lemma 5, $\alpha_i^q, \hat{\alpha}_{i,1}^q,$ and $\hat{\alpha}_{i,2}^q$ are also bounded. According to the triggering law (19) and the boundedness of $\hat{\alpha}_{n,1}^q,$ we can conclude that the implemented event-triggered control input u is bounded. In addition, the inequality $(1/2)\mu_1^2(t) \leq V(t) \leq e^{-kt}V(0) + (C/k)(1 - e^{-kt})$ is obtained by solving $\dot{V} \leq -kV + C.$ Therefore, it is ensured that the tracking error μ_1 converges to a compact set $\Pi = \{\mu_1 \mid |\mu_1| \geq \sqrt{2C/k}\}$ whose size can be adjusted by choosing appropriate design parameters (see Remark 5).

Now, to exclude Zeno behavior, we prove that there exists a minimum inter-event time $t_{\min}.$ Since $|u_e|$ is differentiable except $u_e = 0$ at each triggering instant, we obtain

$$\frac{d}{dt} |\tilde{u}_e| = \frac{d}{dt} (\tilde{u}_e)^{\frac{1}{2}} = \text{sgn}(\tilde{u}_e) \dot{\tilde{u}}_e \leq |\hat{\alpha}_{n,1}^q|. \tag{49}$$

Note that $\hat{\alpha}_{n,1}^q = \hat{\alpha}_{n,2}^q,$ and the uniform boundedness of $\hat{\alpha}_{n,2}^q$ is ensured from the previous analysis. Thus, there exists a positive constant α^* such that $|\hat{\alpha}_{n,1}^q| = |\hat{\alpha}_{n,2}^q| \leq \alpha^*.$ Consequently, according to the proposed triggering law (19), integrating $\frac{d}{dt} |\tilde{u}_e| \leq \alpha^*$ during $t \in [t_l, t_{l+1})$ gives $t_{l+1} - t_l \geq (\theta_1 |\mu_n^q(t)| + \theta_2) / \alpha^* \geq \theta_2 / \alpha^*$ for all $l \in \mathbb{Z}^+.$ That is, the minimum inter-event time can be defined as $t_{\min} \triangleq \theta_2 / \alpha^*.$ \square

3.4. Comparison with the Recent Work

In this section, the proposed control scheme is compared with the recent adaptive quantized feedback control scheme in [14]. In the recent work [14], an adaptive quantized feedback recursive controller was designed for nonlinear systems described by

$$\begin{aligned} \dot{x}_i &= x_{i+1} + g_i(\bar{x}_i), \\ \dot{x}_n &= u + g_n(\bar{x}_n) + \vartheta^\top h(\bar{x}_n), \end{aligned} \tag{50}$$

where $i = 1, \dots, n - 1$, g_j , $j = 1, \dots, n$ and h are known nonlinearities, and ϑ is an unknown parameter vector. Here, the unmatched nonlinear functions g_j should be known and satisfy the Lipschitz conditions with known Lipschitz constants. On the contrary, the proposed controller is designed for system (1) involving completely unknown unmatched nonlinear functions f_j and disturbances d_j . Therefore, no information of the nonlinearities is necessary for designing the proposed quantized feedback controller. To deal with these nonlinearities and disturbances in the quantized feedback recursive control design, we present an adaptive function approximation technique using quantized-states-based adaptation laws (see (14) and (15)) and prove the boundedness between α_j and α_j^q .

On the other hand, the quantized feedback controller in [14] was designed as follows:

$$\begin{aligned} \alpha_j &= -k_j \mu_j^q - g_j^q + \hat{\alpha}_{j-1,2}^q, \\ u &= -k_n \mu_n^q - g_n^q - \hat{\vartheta}^\top h^q + \hat{\alpha}_{n-1,2}^q, \\ \hat{\vartheta} &= \gamma_\vartheta (\mu_n^q h^q - \sigma_\vartheta \hat{\vartheta}), \end{aligned} \tag{51}$$

where $j = 1, \dots, n - 1$, k_j , k_n , γ_ϑ , and σ_ϑ , are design parameters, $\hat{\vartheta}$ is the estimate of ϑ , $g_i^q = g_i(x_1^q, \dots, x_i^q)$, and $h^q = h(x_1^q, \dots, x_n^q)$ for $i = 1, \dots, n$. The definitions of μ_j^q and $\hat{\alpha}_{i-1,2}^q$ are same as ours. It should be emphasized that u in (51) is continuously updated. Therefore, this control scheme increases the load in communication through the controller-to-actuator channel which is unfavorable in practical networked control systems with limited communication resources. In order to reduce this load, we developed our control scheme in an event-driven manner which means that u in (18) is updated only when the triggering condition (19) is satisfied.

In summary, compared with [14], the proposed controller can handle uncertain nonlinear systems with strict-feedback unknown nonlinearities while saving the communication resources by reducing the update of the control input u .

Remark 4. In the existing event-triggered controller design, the existence of the minimum inter-event time is necessary to avoid the Zeno behavior. To prove the existence of this minimum inter-event time, the triggering error signals should generally be differentiable [21–26]. However, the quantized feedback control laws reported in [13,14] were not differentiable because of the quantized state variables. To overcome this problem, we employ the auxiliary first-order low-pass filter (23) for the quantized-feedback-based control law α_n^q in (20). Subsequently, the differentiable signal $\hat{\alpha}_{n,1}^q$ is used in the event-triggered actual control law u in (18). Consequently, the existence of the minimum inter-event time can be ensured by the analysis using (49). This design difficulty comes from the simultaneous handling of the quantized-feedback-based control and event-triggered control.

Remark 5. In the proposed quantized-feedback-based event-triggered tracking scheme, the selection of the design parameters is sufficient conditions. The guidelines for the selection of these parameters are based on the proof of Theorem 1 as follows:

(i) As the level of the quantizer δ in (2) decreases with the performance of digital devices or the communication environment, C can be reduced and thus the convergence bound $\sqrt{2C/k}$ can be reduced.

(ii) As $\gamma_{w,i}$ and $\gamma_{b,i}$, $i = 1, \dots, n$, increase while fixing $\sigma_{w,i}$ and $\sigma_{b,i}$ as small constants, the tuning speed of the estimated parameters \hat{W}_i and \hat{b}_i and k can be increased and thus the bound $\sqrt{2C/k}$ can be reduced.

(iii) The eigenvalues of M_i can be increased by adjusting the filter parameters ζ_i and ω_i , $i = 1, \dots, n$, and the control gains k_i can be increased. Then, the bound $\sqrt{2C/k}$ can be reduced by increasing the control gains k_i .

(iv) Reducing the design parameters η_i helps to reduce C , which subsequently reduces $\sqrt{2C/k}$.

(v) Adjusting the triggering parameters θ_1 and θ_2 manipulates the number of event times along the limited network communication resources in transient and steady-state responses.

4. Simulation Results

In this section, a numerical example and a hydraulic servo system were simulated to validate the proposed quantized-feedback-based adaptive event-triggered control result. For the two simulations, the sampling time t_s was set to $t_s = 2$ ms. Thus, the quantized feedback triggering law (19) was monitored every 2 ms. Furthermore, the tracking performance of the proposed quantized feedback control scheme was compared with that of the previous adaptive quantized feedback control scheme reported in [14]. We show that although the proposed event-triggered control scheme was designed in the presence of unknown nonlinearities, its tracking performance was similar to the performance of the previous continuous controller [14] designed in the presence of known nonlinear functions.

4.1. Example 1

The uncertain third-order strict-feedback systems are considered by

$$\begin{aligned} \dot{x}_i &= x_{i+1} + f_i(\bar{x}_i) + d_i, \\ \dot{x}_3 &= u + f_3(\bar{x}_3) + d_3, \end{aligned} \tag{52}$$

where $i = 1, 2$, $f_1 = 0.5x_1 + 0.7x_1^2$, $f_2 = x_1x_2 + 0.4\sin(x_2)$, $f_3 = e^{-x_3^2}x_1 + x_2x_3$, $d_1 = 0.2\sin(t)$, $d_2 = 0.8\cos(t)$, and $d_3 = 0.7e^{-3t}\sin^2(t)$. For the state quantization, the length of the quantization interval δ was $\delta = 0.005$ and the design parameters for the proposed controller were $k_1 = 5$, $k_2 = 10$, $k_3 = 30$, $\gamma_{w,1} = 10$, $\gamma_{w,2} = 1$, $\gamma_{w,3} = 1$, $\sigma_{w,i} = 0.0000001$, $\gamma_{b,i} = 1.5$, $\sigma_{b,1} = \sigma_{b,2} = 0.6$, $\sigma_{b,3} = 0.9$, $\eta_i = 0.3$, $\omega_1 = 20$, $\omega_2 = 30$, $\omega_3 = 200$, $\zeta_i = 0.707$, $\theta_1 = 10$, and $\theta_2 = 0.5$ where $i = 1, 2, 3$. The reference signal is $r = 0.2\cos(0.7t) + 0.6\cos(1.5t)$ and the initial conditions are $\bar{x}_3(0) = [0.5, 0, 0]^T$, respectively. For the comparison of the simulation results, the controller in [14] was implemented with the same design parameters k_i , ω_j , and ζ_j under the assumption that $f_i(\bar{x}_i)$ and d_i are known where $i = 1, 2, 3$ and $j = 1, 2$.

The tracking results and errors are compared in Figure 2a,b, respectively. In each figure, the upper one is the result of the proposed quantized feedback controller and the lower one is the result of the previous quantized feedback controller [14]. As shown in Figure 2, the quantized feedback tracking performances of both controllers were similar, although the proposed quantized feedback approach considers the unknown nonlinearities and the event-triggered inputs. In Figure 3, \hat{b}_i and \hat{W}_i are depicted where the adaptive parameters were bounded even though the quantized states were used to update them. Figure 4a displays the control signal $\hat{\alpha}_{3,1}^q$ and its triggered signal u . Figure 4b depicts the inter-event times where the maximum inter-event time was 0.3 s which is sixty times longer than the sampling time. The triggering error u_e and the triggering threshold $\theta_1|\mu_3^q| + \theta_2$ are shown in Figure 5a and the cumulative number of triggering instants of ours is displayed in Figure 5b. From Figures 4 and 5, it is shown that the control input u is updated when $|u_e|$ reaches $\theta_1|\mu_3^q| + \theta_2$ and the total number of events is 974 which implies that $6.49\% = \frac{974}{30}t_s \times 100$ of the total sampled data of $\hat{\alpha}_{3,1}^q$ are only transmitted through a communication channel during 30 s. Based on these figures, we can conclude that the tracking of uncertain strict-feedback nonlinear systems can be achieved although the quantized state variables x_i^q , $i = 1, 2, 3$, were used, the control input was intermittently updated via the triggering law (19), and the inherent nonlinearities and disturbances were completely unknown.

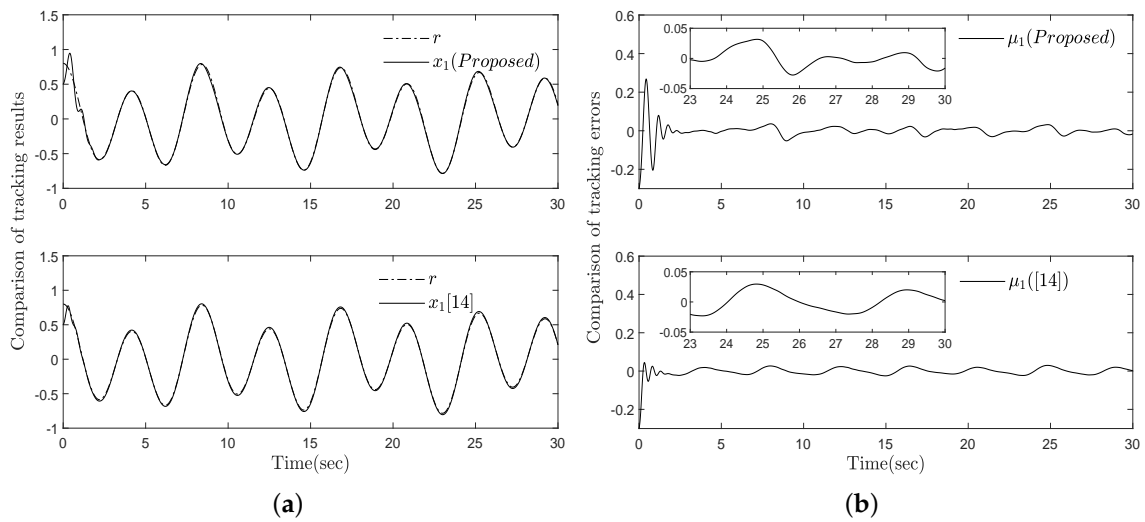


Figure 2. Comparison of tracking results and errors for Example 1 (a) x_1 and r (b) μ_1 .

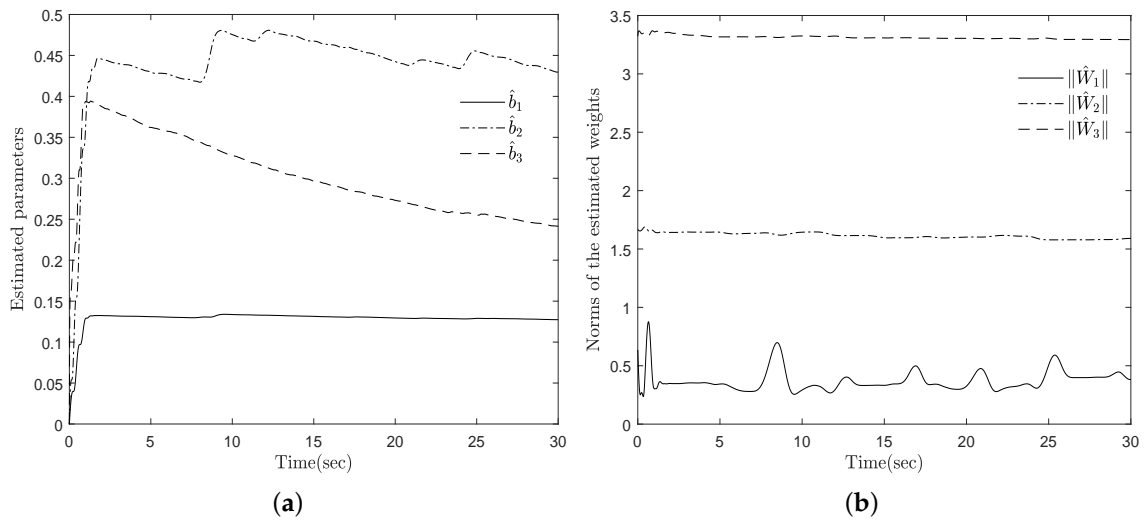


Figure 3. Estimation results of the proposed approach for Example 1 (a) \hat{b}_i (b) $\|\hat{W}_i\|$ for $i = 1, 2, 3$.

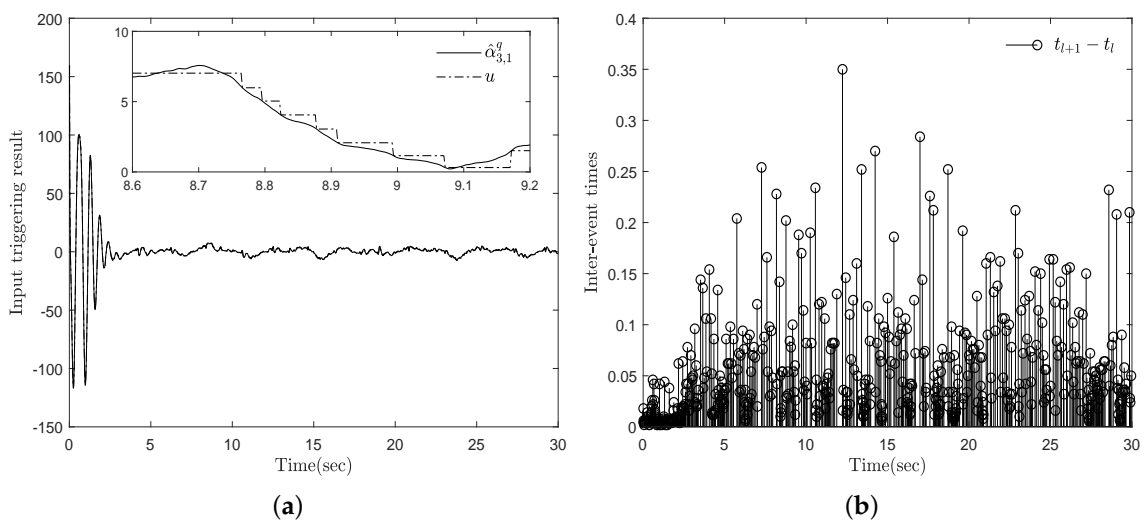


Figure 4. Input triggering result and inter-event times of the proposed approach for Example 1 (a) $\hat{\alpha}_{3,1}^q$ and u (b) $t_{l+1} - t_l$.

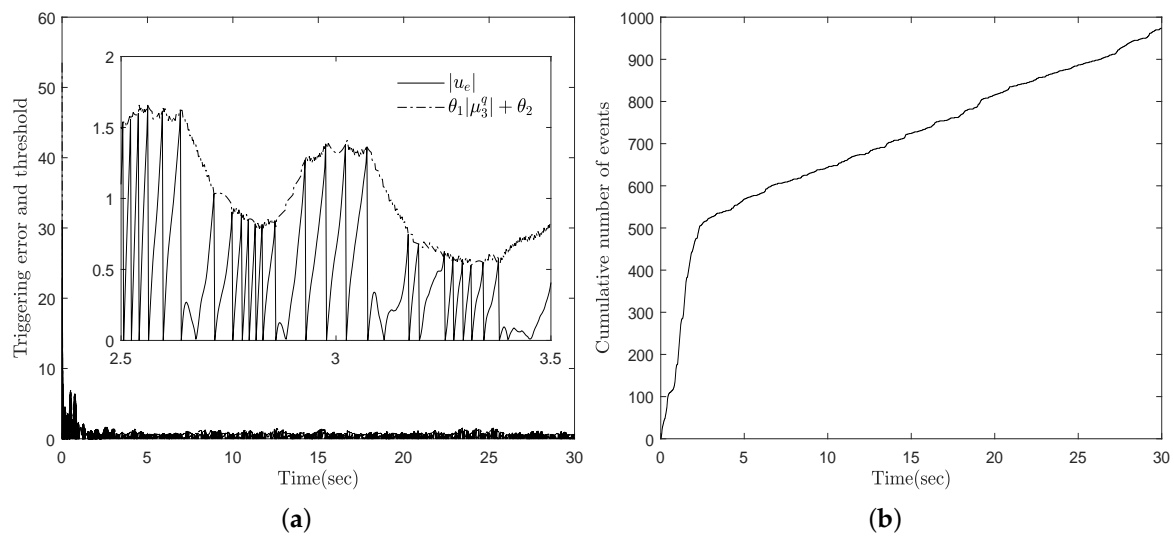


Figure 5. Triggering threshold and the comparison of the cumulative number of events of the proposed approach for Example 1 (a) $|u_e|$ and $\theta_1|\mu_3^q| + \theta_2$ (b) the cumulative number of events.

4.2. Example 2

Consider a servo system driven by a hydraulic actuator where an inertia load is held by a spring-damper and a hydraulic actuator is placed in parallel to the spring-damper. The dynamic model of hydraulic servo systems is described by [34]

$$\begin{aligned}
 m_s \ddot{\vartheta} + b_s \dot{\vartheta} + k_s \vartheta &= F + d, \\
 \frac{V_t}{4\beta_e} \dot{P}_L + C_t P_L + A \dot{\vartheta} &= Q_L,
 \end{aligned}
 \tag{53}$$

where ϑ is the displacement of the inertia load, m_s is the mass of the load, k_s and b_s are the spring constant and the damping constant, respectively, $F = AP_L$ is the driving force produced by the hydraulic actuator; A is the ram area and P_L is the pressure difference of the hydraulic actuator, d denotes the friction inside the cylinder, V_t is the volume of the cylinder, β_e is the effective bulk modulus of oil, C_t is the total internal leakage factor, and Q_L is the supply input flow. For more information about the dynamics of the hydraulic servo systems, see [34].

Let us define the state variables and the control input u as $x_1 = \vartheta$, $x_2 = \dot{\vartheta}$, $x_3 = AP_L/m_s$, and $u = 4A\beta_e Q_L / (m_s V_t)$. Then, (53) can be rewritten by

$$\begin{aligned}
 \dot{x}_1 &= x_2, \\
 \dot{x}_2 &= x_3 + f_2(\bar{x}_2) + d_2(t), \\
 \dot{x}_3 &= u + f_3(\bar{x}_3),
 \end{aligned}
 \tag{54}$$

where $f_2 = -(b_s/m_s)x_2 - (k_s/m_s)x_1$, $d_2 = (1/m_s)d$, and $f_3 = -4(\beta_e/V_t)C_t x_3 - 4(A^2\beta_e/(m_s V_t))x_2$. For the simulation, f_2 , f_3 , and d_2 are assumed to be unknown and the system parameters are set to $m_s = 300$ kg, $b_s = 1500$ N·s/m, $k_s = 9000$ N/m, $A = 1.2656 \times 10^{-4}$ m², $V_t = 6.5312 \times 10^{-3}$ m³, $\beta_e = 6.9861 \times 10^8$ N/m², and $C_t = 4 \times 10^{-13}$ [34]. The friction term is set to $d = \text{sign}(x_2)(20 + 22e^{-100|x_2|})$ N. The reference signal r is given by $r = 0.1 \cos(t)$ and the initial conditions of the state variables are $\bar{x}_3(0) = [0.12, 0, 0]^T$. The design parameters are chosen as $\delta = 0.001$, $k_1 = 5$, $k_2 = 3$, $k_3 = 20$, $\gamma_{w,i} = 30$, $\sigma_{w,i} = 0.00001$, $\gamma_{b,i} = 20$, $\sigma_{b,i} = 0.001$, $\eta_i = 0.5$, $\omega_1 = 10$, $\omega_2 = 70$, $\omega_3 = 150$, $\zeta_1 = \zeta_i = 0.707$, $\theta_1 = 10$, and $\theta_2 = 0.1$ where $i = 2, 3$. Similar to the previous example, the simulation results of the proposed controller are compared with those of the controller in [14] with the same design parameters k_i , ω_j , and ζ_j with $i = 1, 2, 3$ and $j = 1, 2$ and the known information of f_2 , f_3 , and d_2 . In Figure 6, the tracking results and errors are compared where the initial error under the proposed controller converges close to

zero within a few seconds and the tracking performance of the proposed controller is similar to that of the controller in [14]. These figures reveal that the function approximation using quantized states can effectively compensate for the uncertainties f_2, f_3 , and d_2 . In Figure 7, the estimation parameters $\|\hat{W}_i\|$ and $\hat{b}_i, i = 2, 3$ are shown. Figure 8a,b depict the input triggering results and the inter-event times, respectively, under the proposed control scheme. The triggering error and the triggering threshold are demonstrated in Figure 9a and the cumulative number of events is displayed in Figure 9b where the total number of events of ours is 1388. Thus, only $9.25\% = \frac{1388}{30} t_s \times 100$ of the total sampled data of $\hat{a}_{3,1}^q$ during 30 s are released to the communication channel. As illustrated in these figures, we can achieve a good tracking performance for uncertain hydraulic servo systems with state quantization and unknown uncertainties.

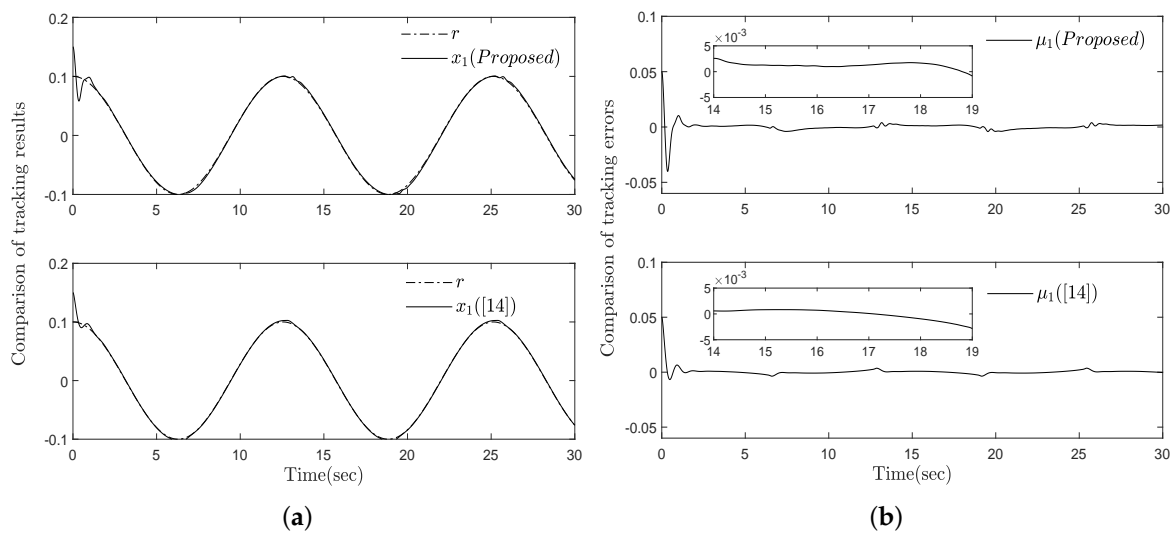


Figure 6. Comparison of tracking results and errors for Example 2 (a) x_1 and r (b) μ_1 .

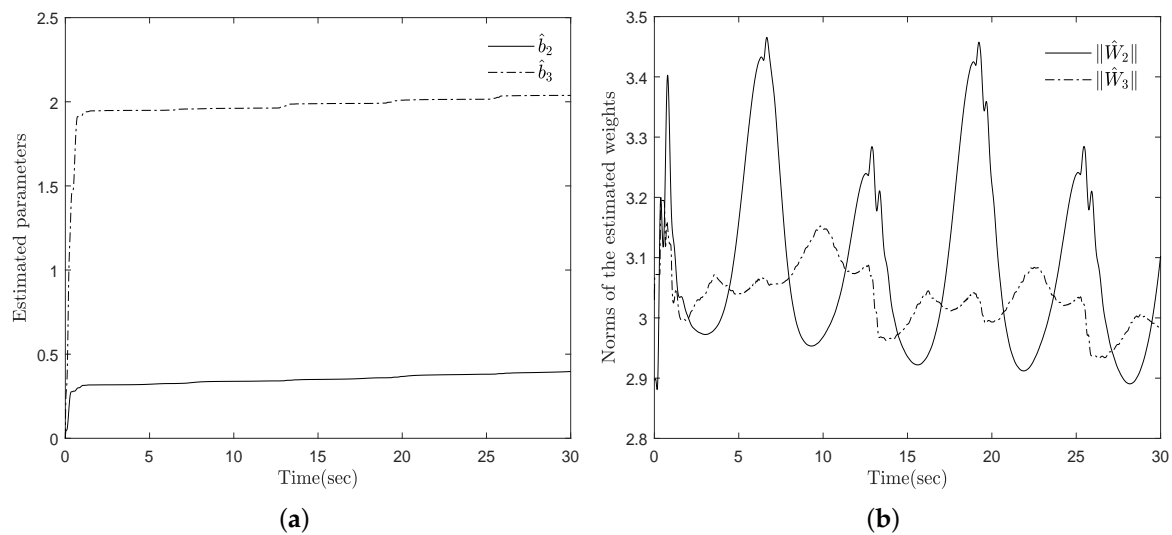


Figure 7. Estimation results of the proposed approach for Example 2 (a) \hat{b}_i (b) $\|\hat{W}_i\|$ for $i = 2, 3$.

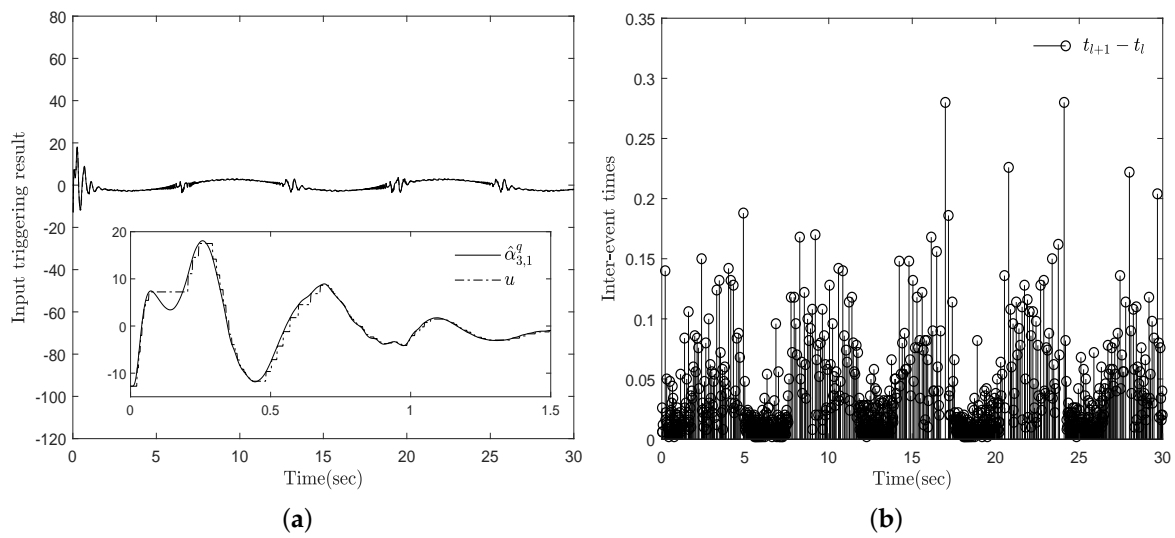


Figure 8. Input triggering result and inter-event times of the proposed approach for Example 2 (a) $\hat{\alpha}_{3,1}^q$ and u (b) $t_{l+1} - t_l$.

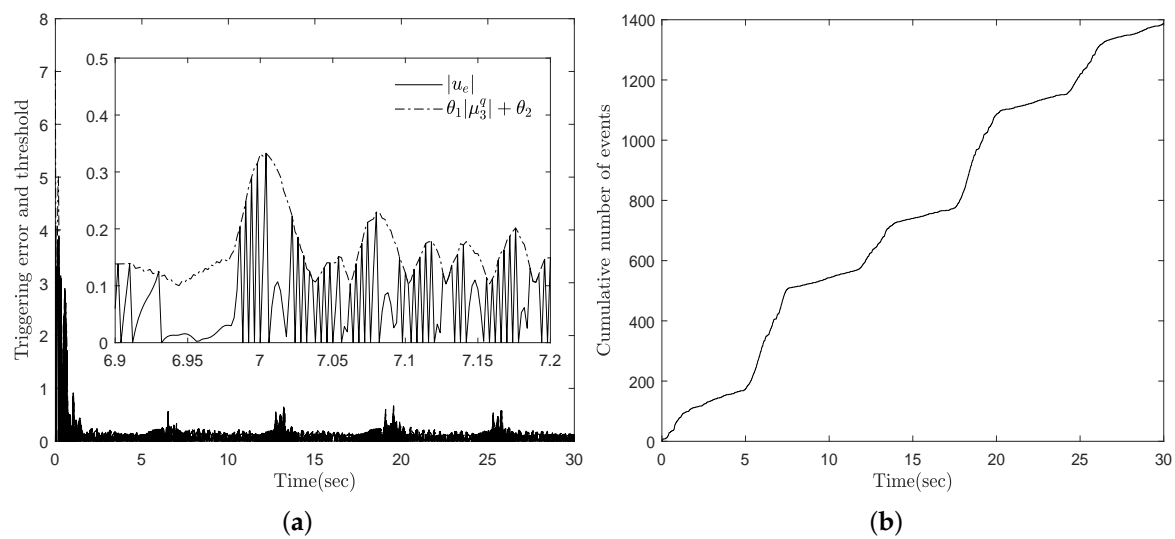


Figure 9. Triggering threshold and the comparison of the cumulative number of events of the proposed approach for Example 2 (a) $|u_e|$ and $\theta_1|\mu_3^q| + \theta_2$ (b) the cumulative number of events.

5. Conclusions

A quantized-feedback-based adaptive event-triggered tracking strategy has been provided for state-quantized nonlinear systems in strict-feedback form with unknown nonlinearities. Different from the existing control methods, an adaptive approximation-based controller has been designed by deriving quantized-states-based adaptive laws and the event triggering issue has firstly been addressed in the quantized feedback control field. The closed-loop stability of the quantized-feedback-based event-triggered recursive control system has been analyzed with three lemmas. Further studies on the quantized-feedback-based adaptive event-triggered tracking problem of robotic systems and nonlinear multi-agent systems are recommended as future works.

Author Contributions: Conceptualization, Formal analysis, methodology, software, writing—original draft preparation, Y.H.C.; Conceptualization, supervision, Validation, writing—review and editing, S.J.Y. All authors have read and agreed to the published version of the manuscript.

Funding: This research was supported by the National Research Foundation of Korea (NRF) grant funded by the Korea government (NRF-2019R1A2C1004898).

Conflicts of Interest: The authors declare no conflict of interest.

References

1. Fu, M.; Xie, L. The sector bound approach to quantized feedback control. *IEEE Trans. Autom. Control* **2005**, *50*, 1698–1711.
2. Elia, N.; Mitter, S.K. Stabilization of linear systems with limited information. *IEEE Trans. Autom. Control* **2001**, *46*, 1384–1400.
3. Montestruque, L.A.; Antsaklis, P.J. Static and dynamic quantization in model-based networked control systems. *Int. J. Control* **2007**, *80*, 87–101.
4. Krstic, M.; Kanellakopoulos, I.; Kokotovic, P.V. *Nonlinear and Adaptive Control Design*; Wiley: New York, NY, USA, 1995.
5. Swaroop, D.; Hedrick, J.K.; Yip, P.P.; Gerdes, J.C. Dynamic surface control for a class of nonlinear systems. *IEEE Trans. Autom. Control* **2000**, *45*, 1893–1899.
6. Farrell, J.A.; Polycarpou, M.; Sharma, M.; Dong, W. Command filtered backstepping. *IEEE Trans. Autom. Control* **2009**, *54*, 1391–1395.
7. Lai, G.; Liu, Z.; Chen, C.L.P.; Zhang, Y. Adaptive asymptotic tracking control of uncertain nonlinear system with input quantization. *Syst. Contr. Lett.* **2016**, *96*, 23–29. [[CrossRef](#)]
8. Xing, L.; Wen, C.; Zhu, Y.; Su, H.; Liu, Z. Output feedback control for uncertain nonlinear systems with input quantization. *Automatica* **2016**, *65*, 191–202.
9. Sui, S.; Tong, S. Fuzzy adaptive quantized output feedback tracking control for switched nonlinear systems with input quantization. *Fuzzy Sets Syst.* **2016**, *290*, 56–78.
10. Huang, L.; Li, Y.; Tong, S. Command filter-based adaptive fuzzy backstepping control for a class of switched non-linear systems with input quantisation. *IET Cont. Theory Appl.* **2017**, *11*, 1948–1958.
11. Xie, K.; Chen, C.; Lewis, F.L.; Xie, S. Adaptive asymptotic neural network control of nonlinear systems with unknown actuator quantization. *IEEE Trans. Neural Netw. Learn. Syst.* **2018**, *29*, 6303–6312.
12. Wang, F.; Zhang, L.; Zhou, S.; Huang, Y. Neural network-based finite-time control of quantized stochastic nonlinear systems. *Neurocomputing* **2019**, *362*, 195–202. [[CrossRef](#)]
13. Zhou, J.; Wen, C.; Wang, W.; Yang, F. Adaptive backstepping control of nonlinear uncertain systems with quantized states. *IEEE Trans. Autom. Control* **2019**, *64*, 4756–4763. [[CrossRef](#)]
14. Choi, Y.H.; Yoo, S.J. Quantized feedback adaptive command filtered backstepping control for a class of uncertain nonlinear strict-feedback systems. *Nonlinear Dyn.* **2020**, *99*, 2907–2918. [[CrossRef](#)]
15. Tabuada, P. Event-triggered real-time scheduling of stabilizing control tasks. *IEEE Trans. Autom. Control* **2007**, *52*, 1680–1685. [[CrossRef](#)]
16. Mazo, M.; Tabuada, P. Decentralized event-triggered control over wireless sensor/actuator networks. *IEEE Trans. Autom. Control* **2011**, *56*, 2456–2461. [[CrossRef](#)]
17. Brockett, R.W.; Liberzon, D. Quantized feedback stabilization of linear systems. *IEEE Trans. Autom. Control* **2000**, *45*, 1279–1289. [[CrossRef](#)]
18. Li, F.; Gao, L.; Dou, G.; Zheng, B. Dual-side event-triggered output feedback H_∞ control for NCS with communication delays. *Int. J. Control Autom. Syst.* **2018**, *16*, 108–119. [[CrossRef](#)]
19. Tallapragada, P.; Chopra, N. On event triggered tracking for nonlinear systems. *IEEE Trans. Autom. Control* **2013**, *58*, 2343–2348. [[CrossRef](#)]
20. Kim, J.H.; Yoo, S.J. Distributed event-triggered adaptive formation tracking of networked uncertain stratospheric airships using neural networks. *IEEE Access* **2020**, *8*, 49977–49988. [[CrossRef](#)]
21. Xing, L.; Wen, C.; Liu, Z.; Su, H.; Cai, J. Event-triggered adaptive control for a class of uncertain nonlinear systems. *IEEE Trans. Autom. Control* **2017**, *62*, 2071–2076. [[CrossRef](#)]
22. Xing, L.; Wen, C.; Liu, Z.; Su, H.; Cai, J. Adaptive compensation for actuator failures with event-triggered input. *Automatica* **2017**, *85*, 129–136. [[CrossRef](#)]

23. Xing, L.; Wen, C.; Liu, Z.; Su, H.; Cai, J. Event-triggered output feedback control for a class of uncertain nonlinear systems. *IEEE Trans. Autom. Control* **2019**, *64*, 290–297. [[CrossRef](#)]
24. Ma, H.; Li, H.; Liang, H.; Dong, G. Adaptive fuzzy event-triggered control for stochastic nonlinear systems with full state constraints and actuator faults. *IEEE Trans. Fuzzy Syst.* **2019**, *27*, 2242–2254. [[CrossRef](#)]
25. Qiu, J.; Sun, K.; Wang, T.; Gao, H. Observer-based fuzzy adaptive event-triggered control for pure-feedback nonlinear systems with prescribed performance. *IEEE Trans. Fuzzy Syst.* **2019**, *27*, 2152–2162. [[CrossRef](#)]
26. Wang, J.; Liu, Z.; Zhang, Y.; Chen, C.L.P. Neural adaptive event-triggered control for nonlinear uncertain stochastic systems with unknown hysteresis. *IEEE Trans. Neural Netw. Learn. Syst.* **2019**, *30*, 3300–3312. [[CrossRef](#)]
27. Li, Y.X.; Yang, G.H. Observer-based fuzzy adaptive event-triggered control codesign for a class of uncertain nonlinear systems. *IEEE Trans. Fuzzy Syst.* **2018**, *26*, 1589–1599. [[CrossRef](#)]
28. Li, Y.X.; Yang, G.H. Adaptive neural control of pure-feedback nonlinear systems with event-triggered communications. *IEEE Trans. Neural Netw. Learn. Syst.* **2018**, *29*, 6242–6251. [[CrossRef](#)]
29. Polycarpou, M.M. Stable adaptive neural control scheme for nonlinear systems. *IEEE Trans. Autom. Control* **1996**, *41*, 447–451. [[CrossRef](#)]
30. Hu, G.D.; Liu, M. The weighted logarithmic matrix norm and bounds of the matrix exponential. *Linear Algebra Its Appl.* **2000**, *390*, 145–154. [[CrossRef](#)]
31. Park, J.; Sandberg, I.W. Universal approximation using radial-basis-function networks. *Neural Comput.* **1991**, *3*, 246–257. [[CrossRef](#)]
32. Wang, C.; Hill, D.J.; Ge, S.S.; Chen, G.R. An ISS-modular approach for adaptive neural control of pure-feedback systems. *Automatica* **2006**, *42*, 625–635.
33. Kurdila, A.J.; Narcowich, F.J.; Ward, J.D. Persistency of excitation in identification using radial basis function approximants. *SIAM J. Control Optim.* **1995**, *33*, 625–642.
34. Na, J.; Li, Y.; Huang, Y.; Gao, G.; Chen, Q. Output feedback control of uncertain hydraulic servo systems. *IEEE Trans. Ind. Electron.* **2020**, *67*, 490–500. [[CrossRef](#)]



© 2020 by the authors. Licensee MDPI, Basel, Switzerland. This article is an open access article distributed under the terms and conditions of the Creative Commons Attribution (CC BY) license (<http://creativecommons.org/licenses/by/4.0/>).